Research Square

Preprints are preliminary reports that have not undergone peer review.
They should not be considered conclusive, used to inform clinical practice,
or referenced by the media as validated information.

Extreme fluid dynamic simulations reveal environmentally-driven morphological features of Euplectella aspergillum

Giacomo Falcucci (giacomo.falcucci@uniroma2.it)
University of Roma Tor Vergata https://orcid.org/0000-0001-6446-4697
Giorgio Amati
SCAI - SuperComputing Applications and Innovation Department, CINECA
Pierluigi Fanelli
University of Tuscia - Viterbo
Vesselin Krastev
University of Rome Tor Vergata
Sauro Succi
Italian Institute of Technology

Physical Sciences - Article

Keywords: Silica Depth Sponge, Amorphous Hydrated Silica, Cylindrical Lattice, Hydrodynamic Fields, Lattice Boltzmann Method, Environmental Physiology

Posted Date: November 16th, 2020

DOI: https://doi.org/10.21203/rs.3.rs-100703/v1

License: This work is licensed under a Creative Commons Attribution 4.0 International License.
Read Full License

Version of Record: A version of this preprint was published at Nature on July 21st, 2021. See the published version at https://doi.org/10.1038/s41586-021-03658-1.

Extreme fluid dynamic simulations reveal environmentally-driven morphological features of *Euplectella aspergillum*

Giacomo Falcucci[1,2], Giorgio Amati[3], Pierluigi Fanelli[4], Vesselin K. Krastev[1] & Sauro Succi[5,2]

[1]*Dept. of Enterprise Engineering "Mario Lucertini" - University of Rome "Tor Vergata"; Via del Politecnico 1, 00133 - Rome - Italy;*

[2]*John A. Paulson School of Engineering and Applied Sciences - Harvard University; 33 Oxford St., 02138 Cambridge (MA) - USA;*

[3]*SCAI - SuperComputing Applications and Innovation Department, CINECA; Via dei Tizii, 6 - 00185 Rome - Italy;*

[4]*DEIM - School of Engineering - University of Tuscia; Largo dell'Università, 01100 Viterbo - Italy;*

[5]*Italian Institute of Technology; P.le Aldo Moro 1, 00185 Rome - Italy*

Due to its remarkable structural properties as well as its tantalising beauty, silica depth sponge *Euplectella aspergillum* has attracted the interest of scientists all over the world since its discovery [1, 2]. Its skeletal system, in fact, is composed of amorphous hydrated silica and it is arranged in a highly regular and hierarchical cylindrical lattice, endowing the whole structure with an amazing flexibility and resilience to damage, [3–7]. In contrast with the major interest in the mechanical properties of the skeletal structure of these *hexatinellida*, the study of the hydrodynamic fields which surround and penetrate the glassy sponge has re-

mained largely unexplored to date, leaving an open question as to the impact of fluid dynamic patterns on *Euplectella*'s environmental physiology. A particularly outstanding question in this respect is whether, besides boosting its tribological characteristics, the structural motifs of *Euplectella* may also respond to an optimisation design in terms of minimising the hydrodynamic stress experienced by the structure. This is precisely the question addressed in the present work. To this purpose, we resort to extreme fluid dynamic simulations based on the Lattice Boltzmann Method [8], featuring of the order of one hundred billion grid points and spanning four spatial decades, from the micro-scale details of the skeleton, all the way up to the full structure of *Euplectella*. Such *in-silico* experiments reproduce the actual living conditions of *Euplectella* [9–11], and prove that the sponge structural elements, not only reduce the overall hydrodynamic stress experienced by the skeletal structure, but also support coherent internal recirculation patterns, arguably feeding the sponge and its host organisms.

The present results open the path towards a new class of numerical investigations at the intersection between fluid mechanics, computational biology and environmental physiology.

The progress in computational science has disclosed unique insights across virtually all fields of science, including the emerging frontier between physics and biology, [12]. The approach to Exa-scale class computational facilities, [14] will enable a further deepening in biological insights and predictions, allowing to explore questions beyond the reach of experimental investigations. As an example, the study of the deep connection between structure and function lies at the core of modern biology, from cell cycles and metabolic analysis, all the way up to entire organs or the overall body of living creatures [13]: the availability of unprecedented computational power is

enabling the study of realistically complex biological models, isolating the influence of different stimuli to the physiology of living organisms. The main of focus of the present work is the study of the fluid dynamic performance of deep-sea sponges in their actual living conditions, reproduced via *in-silico* experiments conducted on one among the top-ten most powerful computational facilities in the world, "Marconi100" [15]. More specifically, leveraging the flexibility and resolution provided by extreme numerical simulations, we have analysed different fluid regimes corresponding to the actual living conditions of deep-sea glassy sponges and we have *disentangled* the morphological characteristics of *Euplectella aspergillum* in order to pin down the specific fluid dynamic role of each of its skeletal features.

Deep-sea glass sponge *Euplectella aspergillum* belongs to the phylum Porifera and to the class of Hexactinellida: it dwells the bottom of the oceans, especially in the Pacific and around Antarctica, at depths of $100 - 1000$ m, where it can make for up to 90% of the whole biomass. Besides their enthralling beauty, these sponges, also known as Venus' flower baskets, are characterised by amazing structural properties, that have sparked the attention of researchers since their discovery [1, 16, 17]. More specifically, the hierarchical arrangement of their skeletal structure has proven to both retard crack propagation and increase buckling strength [6, 18], approaching the optimal material distribution, as recently highlighted in [7].
However, despite the vast scientific literature focused on the tribological properties of *Euplectella*'s skeletal structure, to the best of our knowledge, the study of the actual surrounding and internal hydrodynamics under *in-vivo* conditions has never been charted out, to date.

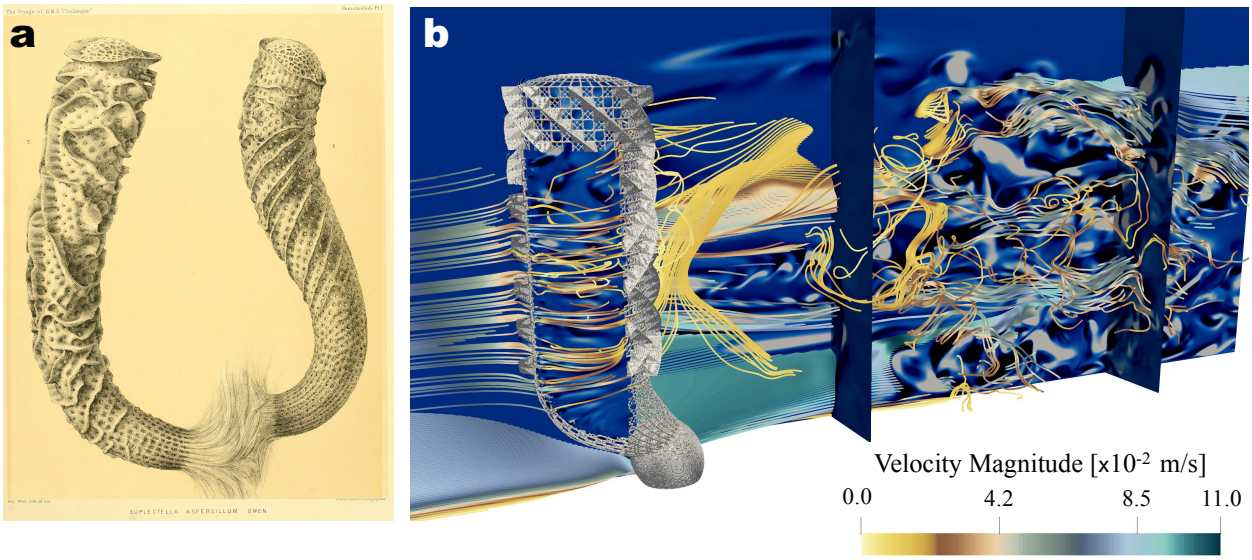

Figure 1: ***Euplectella aspergillum***. **a**: Silica skeleton of the deep-sea sponge *Euplectella aspergillum*, original drawing from [2]; **b**: *Euplectella aspergillum*, reconstructed according to [3], immersed in a hydrodynamic flow at $\mathrm{Re} = 2000$. The panel highlights the contours of helicity $\mathcal{H}$ and the streaklines of the flow, coloured according to the flow velocity magnitude. The presence of vortical structures within the sponge, likely to serve feeding purposes, is apparent. The presence of both *fenestræ* and external ridges on *Euplectella aspergillum* skeleton blow the intermittency connected to the flow regime ($\mathrm{Re} = 2000$) downstream the structure, giving rise to a remarkably $quiescent$ region in the proximity of the sponge.

We have conducted extreme fluid dynamic simulations in order to assess the role of the different skeletal features of a full glassy sponge, in its actual living conditions, reproduced through different values of the water velocity, hence Reynolds number, $\mathrm{Re} = uD/\nu$, where u is the water velocity, D the sponge diameter at its top section (~ 4 cm in our case) and ν is the water kinematic viscosity ($\nu \sim 1.75\ 10^{-6}$ m^2/s at temperatures ranging between 1° and 3° C, [11]).

Starting from the known, average distribution of water velocity in proximity of the bottom of the ocean, which ranges between 0 and $\sim$ 11 cm/s in the first 30 cm over the sea bed [10], we have analysed the flow regimes corresponding to $\mathrm{Re} = 100,\ 500,\ 1000,\ 1500$ and 2000. These simulations provide a unique insight into the potential evolutionary path behind the formation of the external skeleton of *Euplectella aspergillum*, in conjunction with its tribological properties, highlighting at the same time environmental flow-driven *raisons d'être* for the sponge shape and its peculiar structural motifs.

All simulations at $\mathrm{Re} \geq 500$ show clear evidence of vortical flow patterns within the skeletal structure of the sponge, while downstream the hexatinellid, a region of *quiescence* is observed, with the intermittent patterns [20] materialising only several diameters downstream the sponge, in contrast to what happens in the presence of solid obstacles, [21].

More specifically, we report in Fig. 1 a statistical steady state flow configuration for a full *Euplectella aspergillum* sponge at $\mathrm{Re} = 2000$, a typical regime for the living specimen. The complexity of the flow inside and outside the hexatinellid is evicted by means of the contours of helicity ($\mathcal{H} = \vec{u} \cdot \vec{\omega}$, where $\vec{\omega} = \left(\vec{\nabla} \times \vec{u}\right)$ is the local flow vorticity, see Methods Section) and the streaklines coloured according to the magnitude of the flow velocity: the presence of the *quiescent* region extending several diameters downstream the glassy sponge is apparent from our *in-silico* experiments.

To delve deeper into such a peculiar fluid dynamic behaviour and to identify the *Euplectella*'s structural characteristics that eventually trigger it, we have leveraged the flexibility of numerical approaches by *manipulating* the hexatinellid original shape: we realized a fluid dynamic "evo-

lutionary" sequence of geometries morphologically related to the body of *Euplectella*'s skeleton (neglecting the anchoring section to the seabed).

More specifically, we have studied two *solid* geometries, namely a plain cylinder and a cylinder with the same external ridge patterns that decorate *Euplectella*'s skeletal structure, and two *open* geometries, characterised by the presence of holes, or rather *fenestræ* on their surface. All these geometries, reported in Fig. 2(a) are subjected to periodic top and bottom boundaries.

For each geometry, we have simulated the corresponding hydrodynamic field, and studied the downstream intermittency that arises at high Re numbers ($\mathrm{Re} > 100$). We have monitored the time evolution of the fluid velocity $\vec{u}(P,t)$ at a probe P located a distance $\sim 2.5\ D$ downstream the sponge, $\sim D/2$ from the symmetry axes along the flow direction at altitude $H/2$ (H being the height of our computational domain).

Figure 2(a) reports the time evolution of the three cartesian components of the flow velocity $u_x(t), u_y(t), u_z(t)$ at the probe location P. The figure refers to the final $\sim 4\%$ of the time evolution, corresponding to the statistical steady state of the given fluid regime.

Figure 2(a) shows that the two *solid* geometries, namely the cylinder and the cylinder with ridges, are characterised by intense fluctuations of all three velocity components. By contrast, even at $\mathrm{Re} = 2000$, the reticular sponge and the *Euplectella aspergillum* geometries exhibit a dramatic suppression of such fluctuations. Moreover, we found that even at high Reynolds numbers ($\mathrm{Re} \geq 500$), the presence of the *fenestræ* in the open geometries provides a suppression of the z-component of the fluid velocity, leading to a quasi-2D flow in the wake of the sponge (see Fig. 2(a)).

The effect of Re number on the uniformity of the flow field downstream the geometries under

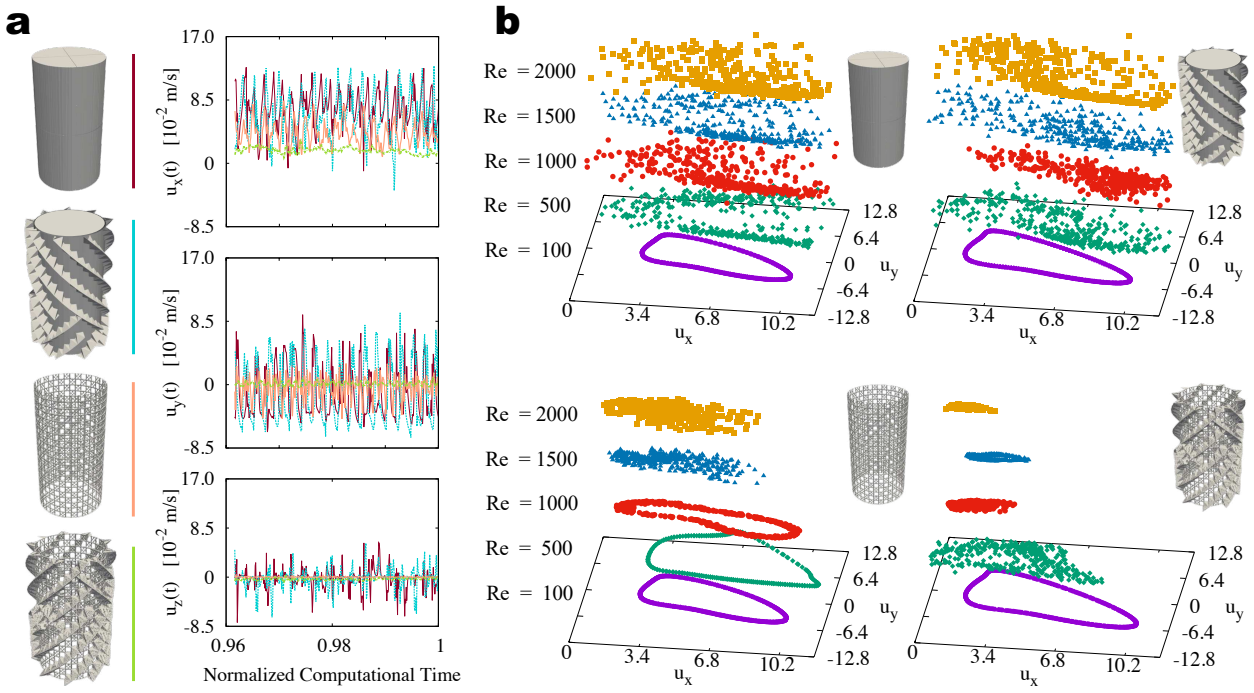

Figure 2: **Analysis of the fluid dynamic "evolutionary" path towards *Euplectella aspergillum***. **a**-left: Sequence of geometries adopted to explore the "evolutionary" path of *Euplectella*. From top to bottom, the two *solid* geometries, namely a plain cylinder and a cylinder with helical decorations, and the two porous ones, with *fenestræ*: a reticular sponge and a reticular sponge with helical decorations. The latter is highly representative of the actual skeletal structure of *Euplectella aspergillum*. **a**-right: Time evolution of the three components of the flow velocity $\vec{u}(P,t)$ where P is a probe located 2.5 diameters downstream the sponge (see main text), at $\mathrm{Re} = 2000$, for the four considered, periodic geometries. It is again apparent that the intermittent three-dimensional fluctuations past the cylinder are nearly totally suppressed for the case of *Euplectella*. The panels report the last $\sim 4\%$ of the whole simulation time span ($2\ 10^5$ out of $5.2\ 10^6$ time steps). **b**: Polar diagrams of the x, y velocity components in cm/s, downstream the solid structure, at the probe P location, for all explored Re regimes. The panel highlights the stabilising effects on the fluid wake, due to the concurrent influence of the *fenestræ* and the ridges of *Euplectella*.

investigation is summarised in Figure 2(b), where the flow pattern exhibits a very visible broken-symmetry.

The two *solid* geometries exhibit the lowest critical Re numbers: the presence of the *fenestræ* in the reticular sponge and in the *Euplectella*'s structure provide a dramatic *stabilising* effect on the flow wake downstream the structure.

Comparison with the circular cylinder at the same Re number, highlights that the *fenestræ* in the skeleton of *Euplectella* play a crucial role in blowing out the intermittency downstream the solid structure, as represented in Fig. 1.

To further corroborate such finding, we have analysed the helicity $\mathcal{H}$ and enstrophy $\omega^2 = |\vec{\nabla} \times \vec{u}|^2$ (see Methods Section) fields for the *Euplectella*, compared to those of the plain cylinder, as reported in Fig. 3.

Panels 3 (a) and (b) show the patterns of $\mathcal{H}$ and ω^2, confirming the presence of a *quiescent* region, downstream the sponge skeletal structure. The results are representative of the statistical steady state reached at $\mathrm{Re} = 2000$, but the same findings are observed in all our simulations with $\mathrm{Re} \geq 500$. The black arrows in the helicity and enstrophy charts in panel 3(b) highlight that the *quiescent* region extends several diameters downstream the skeletal structure of the sponge.

A quantitative assessment of the actual effect of this *quiescent* region downstream the sponge skeleton is obtained by inspecting the drag experienced by the various geometries under inspection.

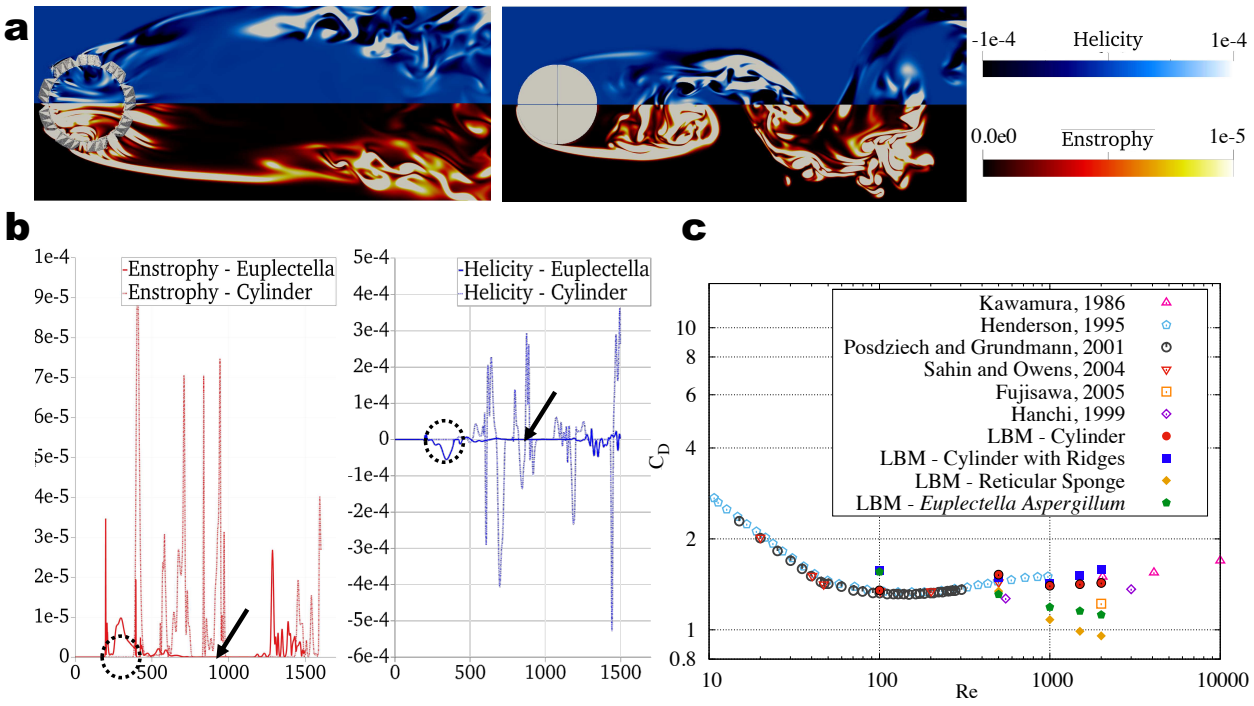

Figure 3: **Effects of *Euplectella* morphology on the hydrodynamic field**. **a**: Comparison of helicity $\mathcal{H}$ and enstrophy ω^2 fields for the *Euplectella* and a plain cylinder, at $\mathrm{Re} = 2000$; **b**: Quantitative comparison between the respective quantities is reported along the x direction in the centerline of the domain. The black arrows in the right panels point to the *quiescent* region that materializes downstream the *Euplectella*'s skeletal structure, due to the presence of the *fenestræ* and the external ridges; **c**: Drag coefficient C_D for the four investigated geometries, compared to the literature values for cylinders, [24–27]. The dramatic drop of C_D in the actual sponge as compared to the *solid* geometries is clearly visible. The trend in C_D also highlights the detrimental effect due to the presence of external ridges, which cause an increase of the drag experienced by the structure, as compared to the reticular sponge, characterised by the presence of *fenestræ* alone.

To this purpose, we compute the drag coefficient C_D:

$$C_D = \frac{2F_{Drag}/A}{\rho_{inlet}\, u_{inlet}^2} \tag{1}$$

in which F_{Drag} is the total (average) drag force acting on the structure, computed at the statistical steady state and along the flow direction; ρ_{inlet} and u_{inlet} are the fluid density and velocity at the domain inlet, respectively, and A is the area of the transverse section of the object, perpendicular to the fluid flow. The values of C_D are reported in Fig. 3(c).

From our analysis, it is apparent that the presence of the *fenestræ* in the *Euplectella*'s skeleton is also beneficial in terms of drag reduction, while the external ridges introduce a systematic increase of the drag experienced by the structure (see Fig. 3(c)). Since drag reduction is clearly a goal for the living organism, which can remain attached to the sea bed with less demanding anchoring structures, the presence of the ridges introduces a new question as to whether they serve just structural purposes. Actually, from the analysis of fluid dynamic results, it emerges that such ridges appear to play a twofold role: first, as already reported in the literature, they contribute to the remarkable mechanical properties of the hexatinellid, [3]; second, they also promote the onset of swirling patterns inside the skeletal structure of the sponge, as highlighted in Figs. 1 and 4. These structures are allegedly acting as the main carriers of feeding functions: upon rotating, they manage to escape dissipation and upon spiralising, they efficiently transport food across the structure of glassy sponge.

To prove such a finding, we have analysed the flow field inside the glassy sponge in terms of the vorticity magnitude and the *Q-criterion*, which defines a vortex as a flow region where $Q = \frac{1}{2}(||\bar{\Omega}||^2 - ||\bar{S}||^2) > 0$, [19, 22, 23] (see Fig. 4 and the Methods Section for more detail).

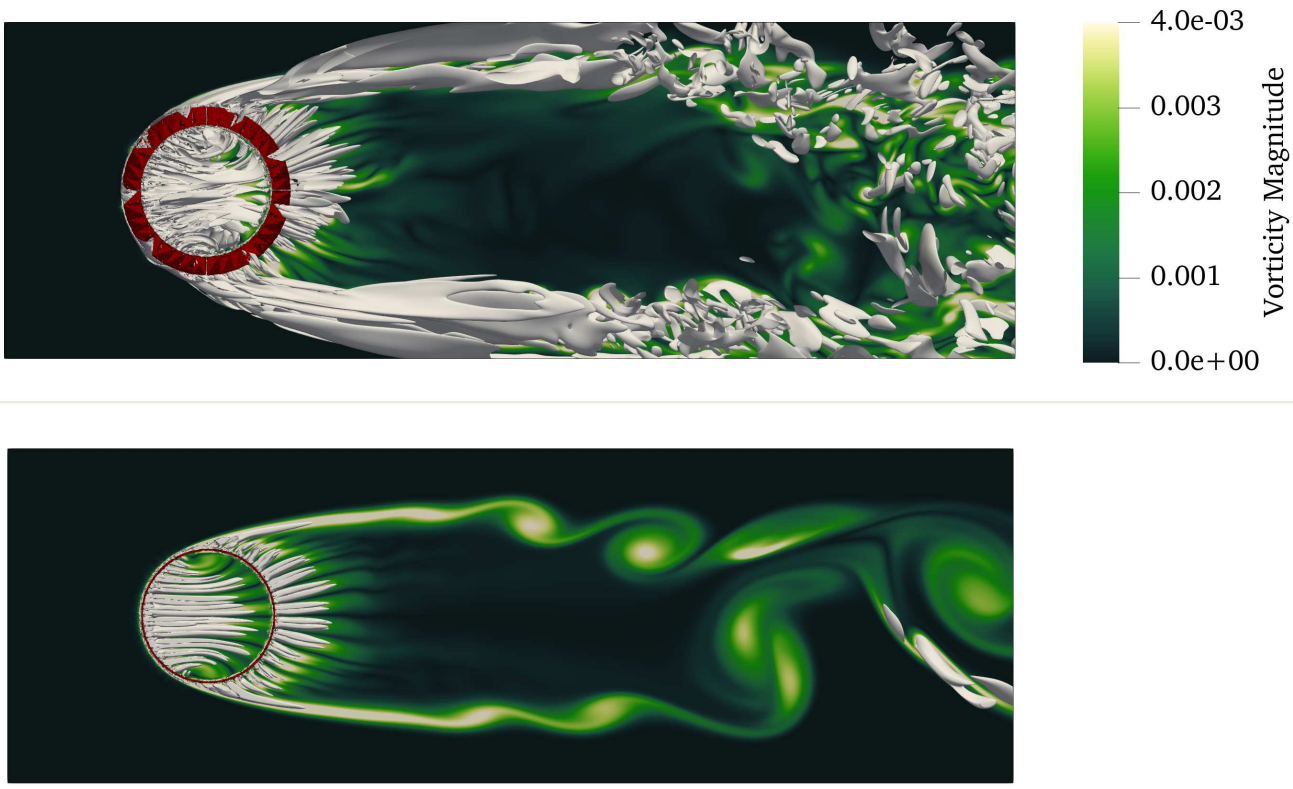

Figure 4: **Vorticity and *Q* structures.** Contours of vorticity magnitude (green palette) and regions characterised by $Q > 0$ (vortical structures). The Figure highlights the fluid dynamic effect of the external ridges in triggering the vortical structures within the *Euplectella*'s skeleton, most likely for feeding purposes.

According to such a criterion, $Q > 0$ implies that the energy connected to local fluid rotation prevails over dissipative phenomena, so that vortical structures may arise within the flow.

Figure 4 provides evidence that within the skeletal structure of the *Euplectella Aspergillum*, the presence of swirling structures is more apparent as compared to the reticular sponge characterised by the presence of *fenestræ* alone, without any external ridges.

This, together with the mapping of the helicity $\mathcal{H}$ within the sponge (see Fig. 3), hints at a strategic fluid dynamic role of such ridges in triggering the spiral patterns within the skeletal structure. Such spiral patterns prove instrumental to feed both the hexatinellid and its host crustacean dwellers.

Discussion

We have found that the skeletal elements of *Euplectella aspergillum*, namely the *fenestræ* and the helical ridges that decorate its surface, are responsible not only for its remarkable structural properties, but also give rise to coherent fluid dynamic phenomena that are aimed to reduce the drag experienced by the sponge, while ensuring a proper circulation within the hexatinellid structure, for feeding purposes. We leveraged the flexibility of numerical simulations in order to isolate the fluid dynamic role of each structural element of *Euplectella aspergillum*: starting from the actual hexatinellid shape, we have analysed a sequence of related morphologies, through an *in-silico* experimental campaign using one of the world-wide leading edge computational facilities, CINECA's "Marconi100".

For all these geometries, we have investigated different flow regimes, starting from the data of water viscosity and velocity distributions at the sea bed, for depths of $100 - 1000$ m, summarised

by the Reynolds numbers $\mathrm{Re} = 100,\ 500,\ 1000,\ 1500$ and 2000.

These simulations have revealed that the hexatienllid's structural elements (known to provide remarkable structural properties) are responsible of reducing the drag experienced by the structure, while triggering vortical patterns for feeding purposes.

More specifically, the presence of the *fenestræ* blows the intermittency rising at flow regimes characterized by $\mathrm{Re} > 100$, several diameters downstream the sponge structure, thereby providing a reduction in the overall drag experienced by the hexatinellid; the helical ridges, while increasing the drag, trigger vortical motions inside the skeletal structure that are important for feeding, while ensuring the well-known structural resistance of the glassy-sponges.

Our results highlight the remarkable effect of environmental conditions on the morphology of the dwellers of the deep ocean, opening the path to novel, inter-disciplinary investigations at the intersection between computational biology, environmental physiology and fluid-structure engineering.

Methods

***Euplectella aspergillum* skeleton reconstruction.** Four main sectors compose *Euplectella*'s skeletal structure: the anchoring section, the connecting section, the main body, and the top section. We have realised a digital mock-up of the whole sponge geometry, as reported in Fig. 1, by accurately reproducing its main structural characteristics.

Excluding the solid anchoring bulb, the remaining sections consist of a periodic structure of two intersecting lattices. The main lattice is composed of axial and circumferential filaments with a diameter of 0.5 mm, orthogonally crossing each other.

A second lattice consists of smaller ligaments, 0.2 mm in diameter and a helical progression around the axial direction. The helices are coupled, each pair at double distance from the previous one. The overall result is a chessboard, with a sequence of crossed and empty boxes. Both lattices envelop a 40 mm diameter cylinder in the main body section, sweeping in a conical-like shape in the connection to the anchoring solid.

On the composed lattice, an aperiodic geometry is placed, which represents the helical outer ridges in the hexatlinellid skeleton.

These prominent ridges mainly follow the helical structure, with a nearly regular repetition also in the actual sponge. They go along the void boxes rows and make a semi-revolution: they turn their spiral direction at random and interrupt or intersect adjacent ridges.

The ridges volume is reproduced with lattice boxes as its basis and spiral edges as the prominent vertex of the solid. The radial protrusion of ridges is placed 5 mm away from the lattice structure.

Simplified models of the main body have been generated (see Fig. 2) for the hydrodynamic investigation, namely: a) a single solid cylinder in place of the lattice structure; b) the same cylinder surrounded by the ridges; c) a cylindrical structure with *fenestræ*; d) the lattice structure surrounded by the ridges.

The Lattice Boltzmann Method and Turbulence Evaluation. The Lattice Boltzmann Method is a numerical technique based on a minimal hydrodynamic formulation of Boltzmann's kinetic Equation, [8, 28, 29].

The fluid fields evolve in time according to the following equation:

$$f_i(\boldsymbol{x} + \boldsymbol{c}_i, t+1) - f_i(\boldsymbol{x}, t) = \omega[f_i^{eq}(\boldsymbol{x}, t) - f_i(\boldsymbol{x}, t)]\,, \tag{2}$$

in which $f_i(\boldsymbol{x}, t)$ represents the probability density function of finding a fluid particle at site $\boldsymbol{x}$ and time t, moving along the i-th lattice direction. In the present work, we employed a nineteen discrete speed ($b = 0, ..., 18$) scheme in three spatial dimensions, also known as D3Q19 lattice, [8]).

The lattice time step Δt and the mesh spacing Δx are taken as the units of time and space, respectively.

The left hand-side of Eq. (2) codes for the free-streaming of fluid molecules, whereas the right-hand side accounts for the collisional relaxation towards the local equilibrium $f_i^{eq}(\boldsymbol{x}, t)$, which takes the form of a second-order low-Mach expansion of a local Maxwell-Boltzmann distribution,

$$f_i^{eq}(\boldsymbol{x}, t) = w_i\, \rho(\boldsymbol{x}, t) \left[1 + \frac{\boldsymbol{c}_i \cdot \boldsymbol{u}(\boldsymbol{x}, t)}{c_s^2} + \frac{(\boldsymbol{c}_i \cdot \boldsymbol{u}(\boldsymbol{x}, t))^2}{2\, c_s^4} - \frac{|\boldsymbol{u}(\boldsymbol{x}, t)|^2}{2\, c_s^2}\right] \tag{3}$$

The relaxation towards local equilibrium is characterised by a time-scale $\tau = 1/\omega = \frac{1}{c_s^2}(\nu + \frac{1}{2})$, ν being the kinematic viscosity of the fluid.

From Eq. 2, one recovers the macroscopic density of the fluid as $\rho(\boldsymbol{x}, t) = \sum_{i=0}^{b} f_i(\boldsymbol{x}, t)$ as well as its velocity $\boldsymbol{u}(\boldsymbol{x}, t) = \sum_{i=0}^{b} \boldsymbol{c}_i\, f_i(\boldsymbol{x}, t)/\rho(\boldsymbol{x}, t)$.

The flow helicity is defined as

$$\mathcal{H}(x,y,z) = \vec{u} \cdot \left(\vec{\nabla} \times \vec{u}\right) = u \left(\frac{\partial w}{\partial y} - \frac{\partial v}{\partial z}\right) + v \left(\frac{\partial u}{\partial z} - \frac{\partial w}{\partial x}\right) + w \left(\frac{\partial v}{\partial x} - \frac{\partial u}{\partial y}\right) \quad (4)$$

while the enstrophy is given by

$$\omega^2(x,y,z) = |\vec{\nabla} \times \vec{u}|^2 = \left(\frac{\partial w}{\partial y} - \frac{\partial v}{\partial z}\right)^2 + \left(\frac{\partial u}{\partial z} - \frac{\partial w}{\partial x}\right)^2 + \left(\frac{\partial v}{\partial x} - \frac{\partial u}{\partial y}\right)^2 \quad (5)$$

The (anti-symmetric) rotation and (symmetric) strain tensors entering the computation of the Q-criterion are defined as follows:

$$\Omega_{ij} = \frac{1}{2}\left[\nabla\vec{u} - (\nabla\vec{u})^T\right] = \frac{1}{2}\left(\frac{\partial u_i}{\partial x_j} - \frac{\partial u_j}{\partial x_i}\right) \quad (6)$$

$$S_{ij} = \frac{1}{2}\left[\nabla\vec{u} + (\nabla\vec{u})^T\right] = \frac{1}{2}\left(\frac{\partial u_i}{\partial x_j} + \frac{\partial u_j}{\partial x_i}\right) \quad (7)$$

Finally, the Q factor, is defined as:

$$Q = \frac{1}{2}\left[||\bar{\Omega}||^2 - ||\bar{S}||^2\right] , \quad (8)$$

where the symbol $||\cdot||$ denotes tensorial norm.

Positive Q's identify flow regions where rotational energy exceeds dissipation, thereby setting the stage for the emergence of vortical structures. High helicity, on the other hand, associates with the presence of three-dimensional spiralizing structures. These structures are the main carriers of feeding functions; upon rotating they manage to escape dissipation, and by spiralizing they manage to transport food across the structure of glassy sponge.

High-Performance-Computing. The simulations have been run on two supercomputing facilities at CINECA, namely "Marconi" and "Marconi100". The former is a *standard* architecture based on CPUs, while the latter, ranking 9th in the May 2020 Top500 list [15], is based on GPU accelerators. The CPU-simulation based exploited 8192 cores, while GPU based simulations have been carried using 64 accelerators to accomplish the "evolutionary" study (thus, in the presence of the periodic geometries), while 512 accelerators have been exploited to study the complete *Euplectella* skeletal structure. The simulations delivered a computational performance of the order of several of Petaflops (10^{15} floating point operations per second), in line with present-day upper-end supercomputers.

We handled up to $4,000$ GPU's, thus collecting up to million cores or processing elements, to manage/analyze and post-process simulation results with about hundred trillions (10^{11}) grid points, demanding about 50 Terabytes of data. All the simulations required about $50,000$ GPU hours and $500,000$ CPU hours.

We wish to emphasise that the excellent scalability of LBM on the aforementioned computational architecture proved absolutely instrumental to enable the full-scale simulation of *Euplectella*, from the micro geometric details, all the way up to the whole size of the sponge.

References

1. Owen, R., Description of a new Genus and Species of Sponge (*Euplectella aspergillum*, O.). *Transactions of the Zoological Society of London*, **3**(2), 203-215 (1849).

2. Report on the scientific results of the voyage of H.M.S. Challenger during the years 1873-76 -

253 under the command of Captain George S. Nares, R.N., F.R.S. and Captain Frank Turle Thom-
254 son, R.N. (1887), https://www.biodiversitylibrary.org/bibliography/
255 6513#/summary.

256 3. Weaver, J.C., Aizenberg, J., Fantner, G.E., Kisailus, D., Woesz, A., Allen, P., Fields, K.,
257 Porter, M.J., Zok, F.W., Hansma, P.K. and Fratzl, P., Hierarchical assembly of the siliceous
258 skeletal lattice of the hexactinellid sponge Euplectella aspergillum. *Journal of Structural Biol-*
259 *ogy*, **158**(1), 93-106 (2007).

260 4. Sundar, V.C., Yablon, A.D., Grazul, J.L., Ilan, M. and Aizenberg, J., Fibre-optical features of
261 a glass sponge. *Nature*, **424**(6951), 899-900 (2003).

262 5. Aizenberg, J., Weaver, J.C., Thanawala, M.S., Sundar, V.C., Morse, D.E. and Fratzl, P., Skele-
263 ton of *Euplectella sp.*: structural hierarchy from the nanoscale to the macroscale. *Science*,
264 **309**(5732), 275-278 (2005).

265 6. Monn, M.A., Weaver, J.C., Zhang, T., Aizenberg, J. and Kesari, H., New functional insights
266 into the internal architecture of the laminated anchor spicules of Euplectella aspergillum. *Pro-*
267 *ceedings of the National Academy of Sciences*, **112**(16), 4976-4981 (2015).

268 7. Fernandes, M.C., Aizenberg, J., Weaver, J.C. and Bertoldi, K., Mechanically robust lattices
269 inspired by deep-sea glass sponges. *Nature Materials*, 1-5 (2020).

270 8. Succi, S., The lattice Boltzmann equation: for complex states of flowing matter. Oxford Uni-
271 versity Press (2018).

9. Kanari, S.-I., Kobayashi, C. and Ishikawa, T., An Estimate of the Velocity and Stress in the Deep Ocean Bottom Boundary Layer, *Journal of the Faculty of Science, Hokkaido University, Series 7, Geophysics*, **9**(1), 1-16 (1991), http://hdl.handle.net/2115/8778.

10. Doron, P., Bertuccioli, L., Katz, J. and Osborn, T.R., Turbulence characteristics and dissipation estimates in the coastal ocean bottom boundary layer from PIV data. *Journal of Physical Oceanography*, **31**(8), 2108-2134 (2001).

11. https://ittc.info/media/4048/75-02-01-03.pdf

12. Kitano, H. Computational systems biology, *Nature* **420**(6912),206-210 (2002).

13. Fung, Y.C., Biomechanics: mechanical properties of living tissues. Springer Science & Business Media (2013).

14. Succi, S., Amati, G., Bernaschi, M., Falcucci, G., Lauricella, M. and Montessori, A. Towards exascale lattice Boltzmann computing. *Computers & Fluids*, **181**, 107-115 (2019).

15. https://www.hpc.cineca.it/hardware/marconi100

16. Chree, C., Recent Advances in our Knowledge of Silicon and of its Relations to Organised Structures. *Nature* **81**, 206–208 (1909).

17. Woesz, A., Weaver, J.C., Kazanci, M., Dauphin, Y., Aizenberg, J., Morse, D.E. and Fratzl, P., Micromechanical properties of biological silica in skeletons of deep-sea sponges. *Journal of Materials Research*, **21**(8), 2068-2078 (2006).

18. Monn, M.A., Vijaykumar, K., Kochiyama, S. and Kesari, H., Lamellar architectures in stiff biomaterials may not always be templates for enhancing toughness in composites. *Nature Communications*, **11**(1), 1-12 (2020).

19. Krastev, V.K., Amati, G., Succi, S. and Falcucci, G., On the effects of surface corrugation on the hydrodynamic performance of cylindrical rigid structures. *The European Physical Journal E*, **41**(8) (2018).

20. Benzi, R., Biferale, L. and Parisi, G., On intermittency in a cascade model for turbulence. *Physica D: Nonlinear Phenomena*, **65**(1-2), 163-171 (1993).

21. Prandtl, L., Applied hydro- & aeromechanics. By: OG Tietjens, Translated by: JP Den Hartog, Dover Publications Inc., New York (1957).

22. Hunt, J. C. R., Wray, A. and Moin, P., Eddies, stream, and convergence zones in turbulent flows. Center for Turbulence Research Report CTR-S88 (1988).

23. Haller, G., An objective definition of a vortex. *Journal of Fluid Mechanics*, **525** (2005).

24. Kawamura, T., Takami, H. and Kuwahara, K., Computation of high Reynolds number flow around a circular cylinder with surface roughness. *Fluid Dynamics Research*, **1**(2), 145 (1986).

25. Hanchi, S., Askovic, R. and Ta Phuoc, L., Numerical simulation of a flow around an impulsively started radially deforming circular cylinder. *International Journal for Numerical Methods in Fluids*, **29**(5), 555-573 (1999).

26. Sahin, M. and Owens, R.G., A numerical investigation of wall effects up to high blockage ratios on two-dimensional flow past a confined circular cylinder. *Physics of Fluids*, **16**(5) (2004).

27. Fujisawa, N., Tanahashi, S. and Srinivas, K., Evaluation of pressure field and fluid forces on a circular cylinder with and without rotational oscillation using velocity data from PIV measurement. *Measurement Science and Technology*, **16**(4), 989 (2005).

28. Krüger, T., Kusumaatmaja, H., Kuzmin, A., Shardt, O., Silva, G. and Viggen, E.M., The lattice Boltzmann method. Springer International Publishing (2017).

29. van den Akker, H. (Ed.), Lattice Boltzmann Modeling for Chemical Engineering (Vol. 55). Academic Press, 2020.

Acknowledgments G.F wishes to acknowledge the CINECA Computational Grant ISCRA-B IsB17 - "SPONGES", id. HP10B9ZOKQ and, partially, the support of PRIN Project CUP E84I19001020006, with Prof. Gino Bella as the Scientific Responsible.

S.S. wishes to acknowledge financial support from the European Research Council under the Horizon 2020 Programme Advanced Grant Agreement n. 739964 ("COPMAT").

Author contributions Giacomo Falcucci devised the research and wrote the original LBM code, in collaboration with Giorgio Amati; G.A. extended the LBM code for massively parallel computation, developed the GPU version for "Marconi100" and helped in collecting and post-processing the data; Pierluigi Fanelli designed all the geometries; G.F. and Vesselin K. Krastev analyzed and post-processed the data; G.F. and Sauro Succi wrote the manuscript. All authors have contributed in analyzing the results of the simulations and in writing and revising the manuscript.

Competing Interests The authors declare that they have no competing financial interests.

Correspondence Correspondence and requests for materials should be addressed to Giacomo Falcucci (email: giacomo.falcucci@uniroma2.it; falcucci@g.harvard.edu).

Figures

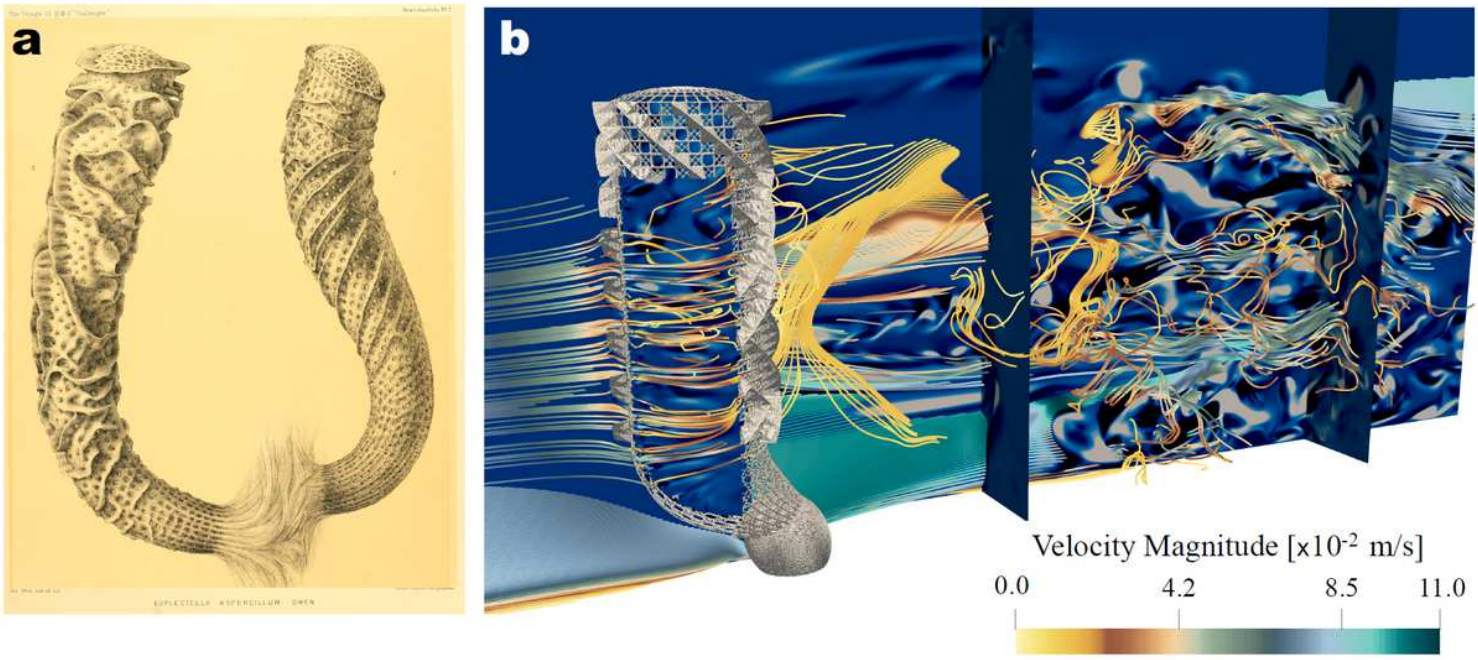

Figure 1

Euplectella aspergillum. a: Silica skeleton of the deep-sea sponge Euplectella aspergillum, original drawing from [2]; b: Euplectella aspergillum, reconstructed according to [3], immersed in a hydrodynamic flow at Re = 2000. The panel highlights the contours of helicity H and the streaklines of the flow, coloured according to the flow velocity magnitude. The presence of vortical structures within the sponge, likely to serve feeding purposes, is apparent. The presence of both fenestræ and external ridges on Euplectella aspergillum skeleton blow the intermittency connected to the flow regime (Re = 2000) downstream the structure, giving rise to a remarkably quiescent region in the proximity of the sponge.

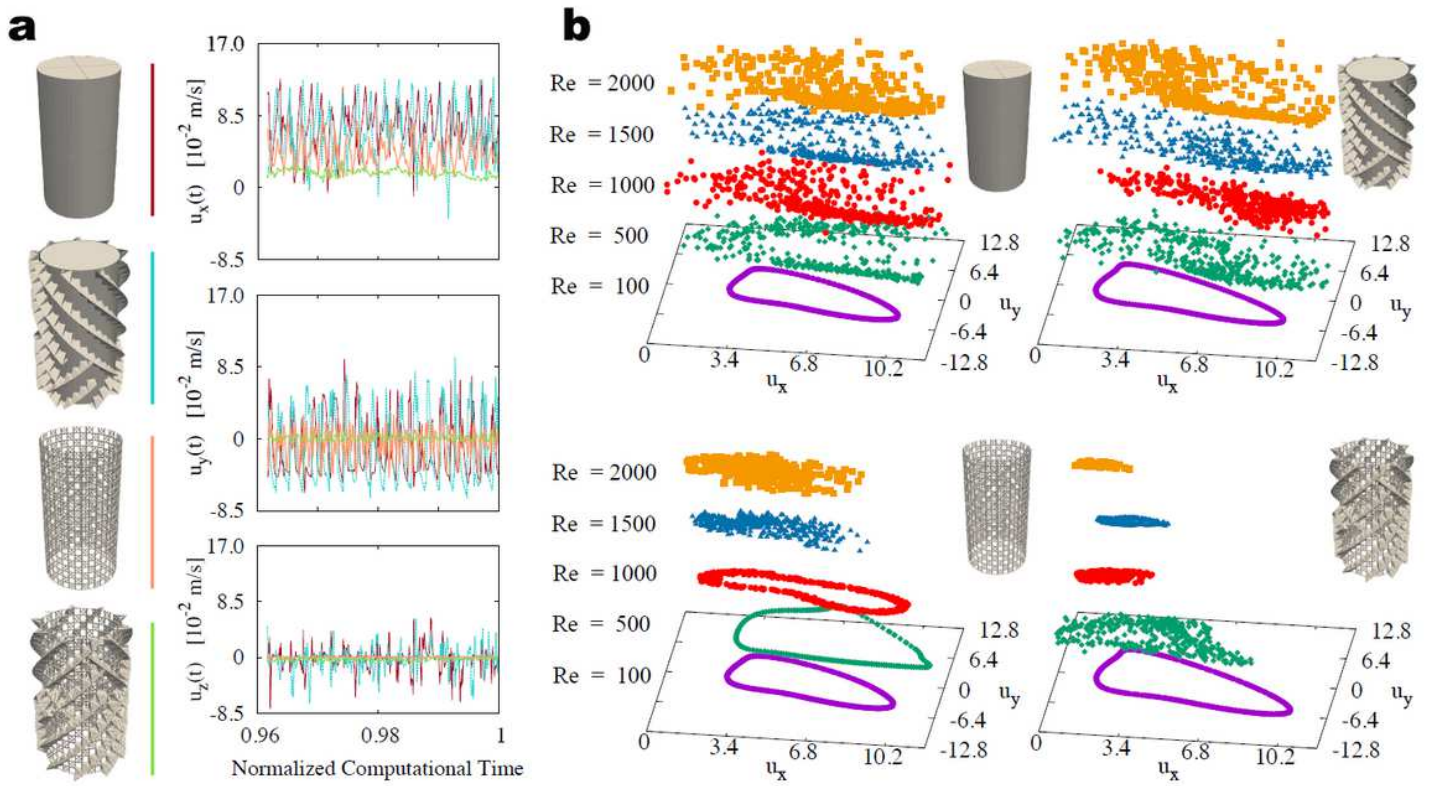

Figure 2

Analysis of the fluid dynamic “evolutionary” path towards Euplectella aspergillum. a-left: Sequence of geometries adopted to explore the “evolutionary” path of Euplectella. From top to bottom, the two solid geometries, namely a plain cylinder and a cylinder with helical decorations, and the two porous ones, with fenestræ: a reticular sponge and a reticular sponge with helical decorations. The latter is highly representative of the actual skeletal structure of Euplectella aspergillum. a-right: Time evolution of the three components of the flow velocity ->u(P; t) where P is a probe located 2:5 diameters downstream the sponge (see main text), at Re = 2000, for the four considered, periodic geometries. It is again apparent that the intermittent three-dimensional fluctuations past the cylinder are nearly totally suppressed for the case of Euplectella. The panels report the last ~ 4% of the whole simulation time span (2 105 out of 5:2 106 time steps). b: Polar diagrams of the x; y velocity components in cm/s, downstream the solid structure, at the probe P location, for all explored Re regimes. The panel highlights the stabilising effects on the fluid wake, due to the concurrent influence of the fenestræ and the ridges of Euplectella.

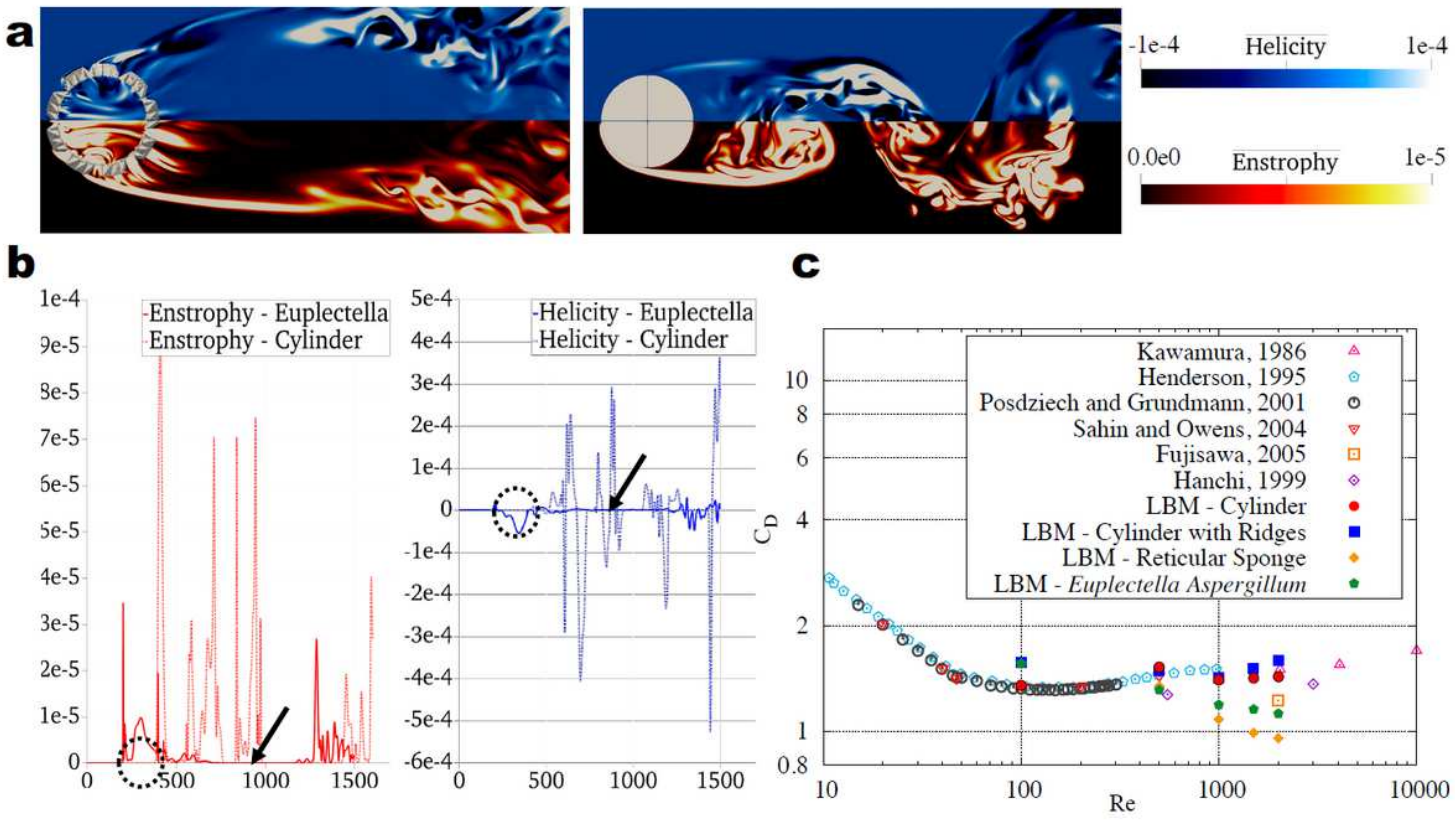

Figure 3

Effects of Euplectella morphology on the hydrodynamic field. a: Comparison of helicity H and enstrophy w2 fields for the Euplectella and a plain cylinder, at Re = 2000; b: Quantitative comparison between the respective quantities is reported along the x direction in the centerline of the domain. The black arrows in the right panels point to the quiescent region that materializes downstream the Euplectella's skeletal structure, due to the presence of the fenestræ and the external ridges; c: Drag coefficient CD for the four investigated geometries, compared to the literature values for cylinders, [24–27]. The dramatic drop of CD in the actual sponge as compared to the solid geometries is clearly visible. The trend in CD also highlights the detrimental effect due to the presence of external ridges, which cause an increase of the drag experienced by the structure, as compared to the reticular sponge, characterised by the presence of fenestræ alone.

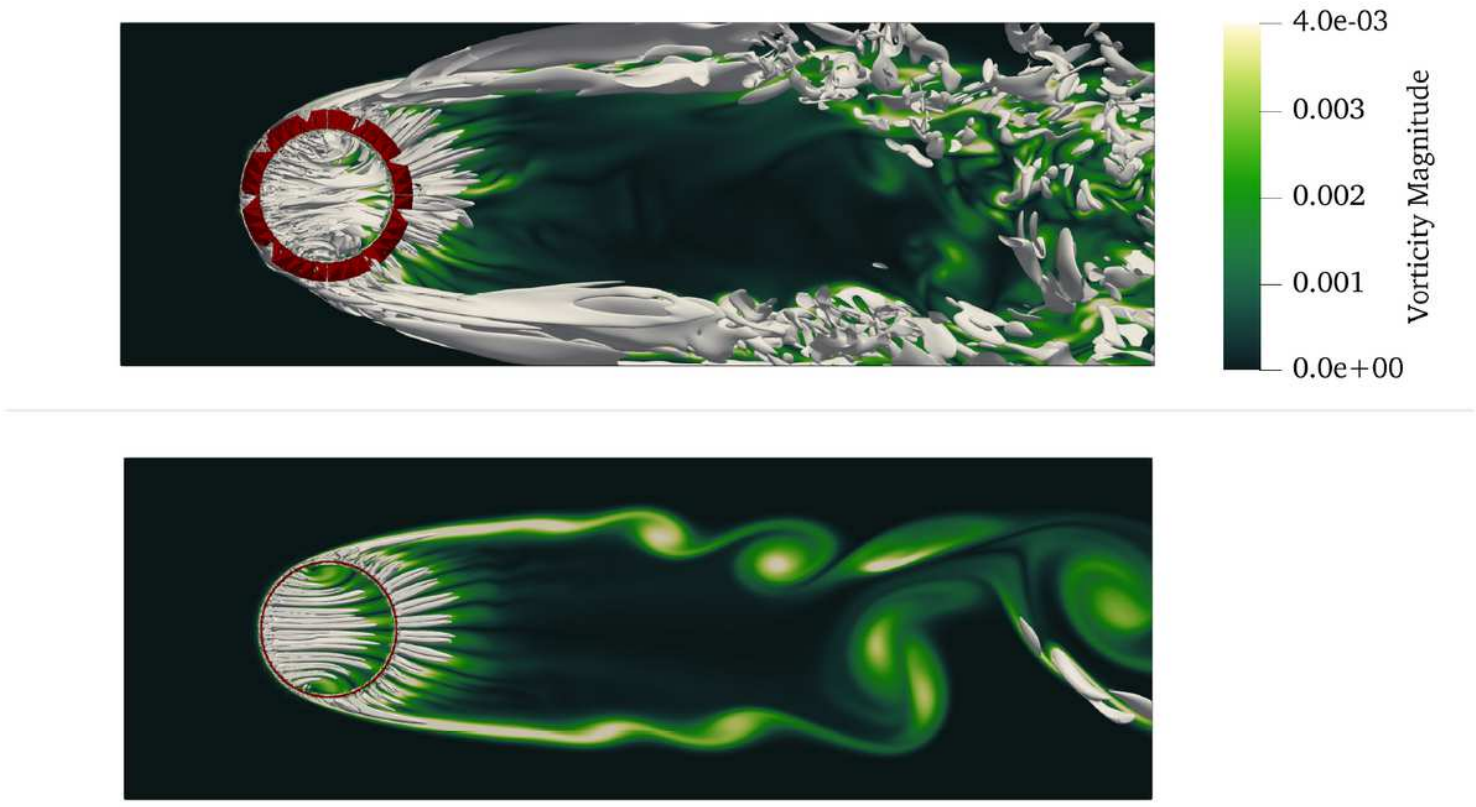

Figure 4

Vorticity and Q structures. Contours of vorticity magnitude (green palette) and regions characterised by Q > 0 (vortical structures). The Figure highlights the fluid dynamic effect of the external ridges in triggering the vortical structures within the Euplectella's skeleton, most likely for feeding purposes.